ISSN 0001-4338, Izvestiya, Atmospheric and Oceanic Physics, 2007, Vol. 43, No. 4, pp. 514–525. © Pleiades Publishing, Ltd., 2007.
Original Russian Text © V.A. Yankovsky, V.A. Kuleshov, R.O. Manuilova, A.O. Semenov, 2007, published in Izvestiya AN. Fizika Atmosfery i Okeana, 2007, Vol. 43, No. 4, pp. 557–569.

# Retrieval of Total Ozone in the Mesosphere with a New Model of Electronic–Vibrational Kinetics of $O_3$ and $O_2$ Photolysis Products

**V. A. Yankovsky, V. A. Kuleshova, R. O. Manuilova, and A. O. Semenov**

*Fock Institute of Physics, St. Petersburg State University, ul. Ul'yanovskaya 1, Petrodvorets, St. Petersburg, 198504 Russia*
*e-mail: Valentine.Yankovsky@paloma.spbu.ru*

Received December 6, 2006

**Abstract**—The paper presents a new model of electronic–vibrational kinetics of the products of ozone and molecular oxygen photodissociation in the terrestrial middle atmosphere. The model includes 45 excited states of the oxygen molecules $O_2(b^1\Sigma_g^+, v = 0–2)$, $O_2(a^1\Delta_g, v = 0–5)$, and $O_2(X^3\Sigma_g^-, v = 1–35)$ and of the metastable atom $O(^1D)$ and over 100 aeronomic reactions. The model takes into account the dependence of quantum yields of the production of $O_2(a^1\Delta_g, v = 0–5)$ in a singlet channel of ozone photolysis in the Hartley band on the wavelength of photolytic emission. Taking account of the electronic–vibrational kinetics is important in retrieval of the vertical profiles of ozone concentration from measured intensities of the Atm and IR Atm emissions of the oxygen bands above 65 km and leads to an increase in the ozone concentration retrieved from the 1.27-μm emission, in contrast to the previous model of pure electronic kinetics. Sensitivity analysis of the new model is made for variations in the concentrations of atmospheric constituents ($[O_2]$, $[N_2]$, $[O(^3P)]$, $[O_3]$, $[CO_2]$), the gas temperature, rate constants of the reactions, and quantum yields of the reaction products. A group of reactions that most strongly affect the uncertainty of ozone retrieval from measured intensities of atmospheric emissions of molecular oxygen $O_2(b^1\Sigma_g^+, v)$ and $O_2(a^1\Delta_g, v)$ has been determined.

**DOI:** 10.1134/S0001433807040135

## 1. INTRODUCTION

The development of the model of electronic–vibrational kinetics of the products of ozone and oxygen photolysis at the Laboratory of Middle and Upper Planetary Atmospheres, St. Petersburg State University, has its own prehistory [1, 2]. An experimental group under the leadership of L.E. Khvorostovskaya on the study of aeronomic reactions in laboratory conditions was organized at the Department of Atmospheric Physics, Leningrad State University (now St. Petersburg State University), in the late 1960s. An experimental facility was designed on the basis of oxygen glow discharge. The weakly ionized plasma of glow discharge is similar in characteristics to the lower thermosphere of the Earth. The abundance of ozone, metastable molecules $O_2(a^1\Delta_g)$ and $O_2(b^1\Sigma_g^+)$, and oxygen atoms in the $O(^3P)$, $O(^1D)$, and $O(^1S)$ states reached 0.001–10% of the abundance of $O_2$ molecules. This circumstance allowed the rate constants of individual aeronomic reactions with the involvement of these components to be measured depending on the gas temperature and average energies of electrons and atoms. For analysis of photochemical mechanisms of production of the excited $O_2$ and $O(^1S)$ atoms, in the Earth's and Venus's atmospheres a series of experiments have been conducted. The kinetics of ozone in oxygen glow discharge was investigated in [3]. Ozone was shown to be produced in an atmospherically typical triple reaction in the collision between $O_2$ and $O(^3P)$, and collisions with the $O(^3P)$ atoms played a dominant role in $O_3$ destruction. The ozone concentration was determined by measuring the absorption of radiation of a standard UV source in the Hartley band. In [4, 5], the temperature dependence of the rate constant of the energy transfer from $O(^1D)$ atoms to excited $O_2(b^1\Sigma_g^+)$ molecules during collisions with $O_2$ molecules was investigated in a wide temperature range (345–605 K). Further experiments [6] have shown that a dominant process in this reaction is the transfer of excitation to the electronic–vibrational levels of the oxygen molecule:

$$O(^1D) + O_2(X^3\Sigma_g^-, v = 0) \longrightarrow O_2(b^1\Sigma_g^+, v \le 2) + O(^3P). \quad (1)$$

In [6], the mechanism of the electronic–vibrational relaxation of $O_2(b^1\Sigma_g^+, v)$ in a pure oxygen atmo-

sphere was investigated in the temperature range 340–445 K, rate constants were measured for the reactions $O_2(b^1\Sigma_g^+, v = 2) + O_2(X^3\Sigma_g^-, v = 0) \longrightarrow$ ($k = 3.15 \times 10^{-12}$ cm$^3$ s$^{-1}$), $O_2(b^1\Sigma_g^+, v = 2) + O(^3P) \longrightarrow$ ($k = 1.1 \times 10^{-11}$ cm$^3$ s$^{-1}$), and $O_2(b^1\Sigma_g^+, v = 2) + O_3 \longrightarrow$ ($k = 2.9 \times 10^{-10}$ cm$^3$ s$^{-1}$), estimates of rate constants of analogous reactions with $O_2(b^1\Sigma_g^+, v = 1)$ were made, and a photochemical model was first proposed for calculating vertical profiles of $O_2(b^1\Sigma_g^+, v = 1, 2)$ in the altitude range 85–120 km of the terrestrial atmosphere in daylight. Note that rate constants of these reactions were measured for the first time. Ten years later, some of these results were confirmed with the use of another method, the laser pumping of levels [7, 8]. Data of our laboratory [4–6] and of the scientific teams from Space Research Institute International (California) [7] and the Jet Propulsion Laboratory [9] allowed us in 2003 to develop an electronic–vibrational kinetics model of the products of ozone and molecular oxygen photolysis in the middle atmosphere, named the YM-2003.

In [1], analysis of the data obtained from a rocket mission as part of the METEORS program [10], in which vertical profiles of the Atm (762 nm) and IR Atm (1.27 μm) emissions in the bands of molecules $O_2(b^1\Sigma_g^+, v = 0)$ and $O_2(a^1\Delta_g, v = 0)$, respectively, were simultaneously measured, has shown that only the model of electronic–vibrational kinetics of ozone and molecular oxygen photolysis can provide consistent vertical ozone profiles retrieved from these two simultaneously measured emissions. The discrepancy between the retrieved ozone profiles in the altitude range 65–95 km does not exceed 6% in the model of electronic–vibrational kinetics of oxygen and molecular photolysis (YM-2003 from [1]) and reaches 30% in the model of pure electronic kinetics [11], which will be referred to as the MSZ model. Nevertheless, the interpretation of the experiments on the retrieval of vertical ozone profiles from emissions from the states $O_2(b^1\Sigma_g^+, v = 0)$ and $O_2(a^1\Delta_g, v = 0)$ is still being performed within the framework of pure electronic kinetics.

In the first version of the YM-2003 model [1], in accordance with the level of knowledge at that time, the quantum yield of the electronically–vibrationally excited $O_2(a^1\Delta_g, v = 0–5)$ molecules in ozone photolysis in the Hartley band was calculated integrally over the entire band. After the publication of [1], systematic data have appeared on the spectral dependence of quantum yields of electronically–vibrationally excited $O_2(a^1\Delta_g, v = 0–5)$ molecules [7]. In order that these data be taken into account correctly, we included the SOLAR 2000 solar irradiance model in the new version of the YM-2003 model and constructed analytical approximations of quantum yields of electronically–vibrationally excited $O_2(a^1\Delta_g, v = 0–5)$ molecules depending on the wavelength and vibrational number for the entire Hartley band. In addition, constant rates have been first measured in a laboratory experiment for several reactions having an important role in the YM-2003 model: $O_2(b^1\Sigma_g^+, v = 1) + O \longrightarrow$, $O_2(a^1\Delta_g, v = 1, 2) + O_2 \longrightarrow$, and $O_2(X^3\Sigma_g^-, v = 2, 3) + O_2 \longrightarrow$ [7, 8]. All these findings have led us to the development of a new, revised version of the YM-2003 model, which will be referred to as YM-2003 after the date of its first publication.

In this paper, we give a brief description of the new modules of the YM-2003 model and for the first time demonstrate its capabilities for the retrieval of vertical ozone profiles from measurements of altitude profiles of the IR Atm intensity of the $O_2$ band, which are performed on slant paths in the TIMED-SABER satellite experiment.

## 2. YM-2003 MODEL OF ELECTRONIC–VIBRATIONAL KINETICS OF THE PRODUCTS OF OZONE AND OXYGEN PHOTOLYSIS

A detailed scheme of the photodissociation of ozone and molecular oxygen in the YM-2003 model taking into account the population and quenching of all of the electronically–vibrationally excited levels of the oxygen molecules and the $O(^1D)$ atom included in the model is shown in Fig. 1. The scheme displays the photodissociation of $O_2$ in the Schumann–Runge continuum ($J_{SRC}$) and in the hydrogen Lyman-α line $J_{Ly\text{-}\alpha}$, $O_3$ photodissociation in the Hartley ($J_H$), Huggins ($J_{Hu}$), and Chappuis ($J_{Ch}$) bands; resonance photon population of the levels $O_2(b^1\Sigma_g^+, v = 0, 1, 2)$ and $O_2(a^1\Delta_g, v = 0)$ at rates $g_A$, $g_B$, $g_\gamma$, and $g_{IR}$, respectively; the energy transfer between levels by inelastic collisions with $N_2$, $O_2$, O, and $CO_2$ molecules; and radiative quenching.

The updated version of the YM-2003 model for the first time includes the photodissociation of $O_3$ in the Wulf band ($J_{Wulf}$), kinetics of the population of the upper vibrationally excited levels of $O_2(X^3\Sigma_g^-, v \le 35)$, and a two-quantum quasi-resonance energy transfer in the reaction $O_2(X^3\Sigma_g^-, v) + N_2 \longrightarrow O_2(X^3\Sigma_g^-, v - 2) + N_2(X, v = 1)$. In our paper, the base of the rate constants of more than 100 reactions used in the YM-2003 model will not be discussed, because this base was described in detail in [2]. The present paper uses overviews [7, 9, 12] and our laboratory data systematized

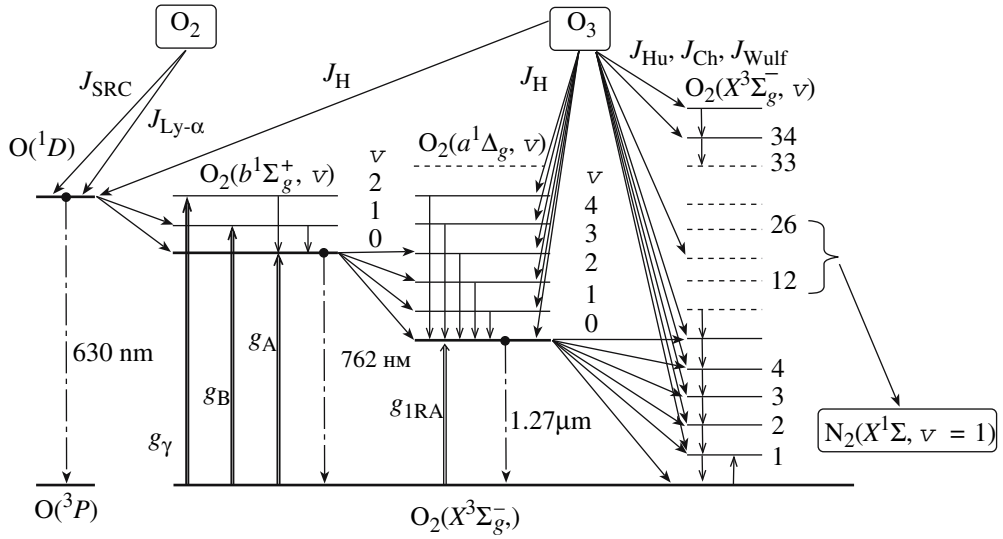


**Fig. 1.** Scheme of the population and quenching of electronically–vibrationally excited levels of molecular oxygen and O($^1D$) atoms in the terrestrial middle atmosphere within the framework of the YM-2003 model.

in [2, 5, 6]. The most significant change was introduced into the module of calculation of the $O_2$ and $O_3$ photodissociation rates.

### *2.1. Module for Calculation of the $O_2$ and $O_3$ Photodissociation Rates*

The rate $g$ of formation of the excited products of the photolysis of $O_2$ and $O_3$, denoted by a symbol $M$, is determined at the altitude $z$ by the formula

$$g(z) = [M(z)] \int_{130}^{850} \beta_\lambda F_\lambda(\infty)\sigma_\lambda e^{-\tau_\lambda(z)} d\lambda, \qquad (2)$$

where $[M]$ is the concentration of the $O_2$ or $O_3$ molecules, $\beta_\lambda$ is the quantum yield of the excited products at the wavelength $\lambda$, $F_\lambda(\infty)$ is the density of the solar radiation flux at the top of the atmosphere, $\sigma_\lambda$ is the absorption cross section for $O_2$ or $O_3$, and $\tau_\lambda$ is the optical thickness of the atmosphere in the direction toward the Sun. The wavelength range (130–850 nm) was divided into 159 sufficiently narrow spectral intervals $\Delta\lambda$ so that the integral in (2) could be replaced within reasonable accuracy with the sum over all intervals by taking the mean $\bar{\beta}_{\Delta\lambda}$, $\bar{\sigma}_{\Delta\lambda}$, and $\bar{\tau}_{\Delta\lambda}$ outside the integral sign in each $\Delta\lambda$. In partitioning the wavelength range into intervals $\Delta\lambda$, we took into account the fact that the quantum yields of some products of ozone photolysis depend on threshold wavelengths (Table 1 below):

$$g(z) = [M(z)] \sum_{\Delta\lambda,} \bar{\beta}_{\Delta\lambda} J_{\Delta\lambda}(z), \qquad (3)$$

where

$$J_{\Delta\lambda}(z) = F_{\Delta\lambda}(\infty)\bar{\sigma}_{\Delta\lambda} e^{-\bar{\tau}_{\Delta\lambda}(z)} \qquad (4)$$

is the rate of photodissociation of $O_2$ or $O_3$ molecules in the $\Delta\lambda$ interval and

$$F_{\Delta\lambda}(\infty) = \int_{\Delta\lambda} F_\lambda(\infty) d\lambda \qquad (5)$$

is the integral flux of solar radiation at the top of the atmosphere in the $\Delta\lambda$ interval.

The values of $F_{\Delta\lambda}(\infty)$ are taken from the SOLAR 2000 model [13, 14]. This model computes daily mean fluxes of solar radiation with a step of 1 nm for wavelengths shorter than 630 nm and a step of 2 nm for 630–850 nm for a given date with consideration for variations in solar activity. Absorption cross sections of molecular oxygen are borrowed from [15] for

**Table 1.** Threshold wavelengths used for calculation of the parameter $x_v$ and normalization factors $C_v$

| Products of $O_3$ photolysis | $O_2(a^1\Delta_g, 0)$ | $O_2(a^1\Delta_g, 1)$ | $O_2(a^1\Delta_g, 2)$ | $O_2(a^1\Delta_g, 3)$ | $O_2(a^1\Delta_g, 4)$ | $O_2(a^1\Delta_g, 5)$ |
|---|---|---|---|---|---|---|
| Threshold $\lambda$, nm | 310 | 296 | 284 | 273 | 263 | 254 |
| $x_v$ | 0.937 | 0.689 | 0.576 | 0.483 | 0.407 | 0.339 |
| $C_v$ | 1.068 | 1.233 | 0.564 | 0.375 | 0.377 | 0.473 |

the Schumann–Runge continuum (130–175 nm), from [16, 17] for the Herzberg continuum (192–240 nm), and from the parametrization of [18] for the hydrogen Lyman-α wavelength (121.6 nm). For calculation of the absorption of radiation by molecular oxygen in the Schumann–Runge bands (175–204 nm), the parametrization of [17] is used with consideration for a partial overlap of these bands by the Herzberg continuum. The absorption cross sections of ozone are taken from [16] for the Hartley band (175–307 nm) and Huggins band (307–362 nm) and from [19] for the Chappuis and Wulf bands (410–850 nm). The optical thickness $\tau_{\Delta\lambda}$ is determined by taking into account the sphericity of atmospheric layers with a vertical step of 1 km. The sphericity effect is most significant at large solar zenith angles (above 80°).

In a direct problem, the vertical profiles of the concentration of atomic oxygen are taken from the model described in [20]. To obtain ozone profiles, a theoretical profile from [21] was joined (from above) with the profiles from [22] (from below) at an altitude of about 86 km. The profiles of molecular oxygen and atmospheric temperature are adopted from the MSISE-90 model [23]. In the inverse problem (retrieval of the vertical ozone profile), the profiles of atomic and molecular oxygen and atmospheric temperature are taken from the corresponding experiments (e.g., SABER; see below).

### *2.2. Quantum Yields of Electronic–Vibrational Molecules $O_2(a^1\Delta_g, v = 0–5)$ as a Function of Wavelength in $O_3$ Photodissociation in the Hartley Band*

In the population of $O_2(a^1\Delta_g, v)$, ozone photolysis in the Hartley band has an important role, especially at altitudes below the mesopause:

$$O_3 + h\nu \longrightarrow O_2(a^1\Delta_g, v = 0–5) + O(^1D). \quad (6)$$

In the MSZ model, this process was assumed to produce only $O_2(a^1\Delta_g, v = 0)$. However, in the Hartley band cross-section peak (254 nm), 56% of molecules are formed in the states $O_2(a^1\Delta_g, v \geq 1)$ [7]. The dependence of quantum yields of the production of $O_2(a^1\Delta_g, v = 0–5)$ molecules by ozone photolysis in the Hartley band $\beta(a, v)$ on the wavelength of photolytic radiation has been used for the first time in the electronic–vibrational kinetics model YM-2003 [24]. Laboratory measurements of the quantum yields of $O_2(a^1\Delta_g, v)$ in reaction (6) have already been performed for more than 25 years. In [24], these measurements have been systematized and a procedure has been proposed for the derivation of analytical expressions for calculating quantum yields of $O_2(a^1\Delta_g, v)$ in ozone photolysis in the Hartley band.

In the paper, this approach is used to calculate quantum yields of $O_2(a^1\Delta_g, v)$ for levels with the vibrational number $v \leq 5$. A specific feature of photodissociation is that there is a threshold wavelength at which oxygen molecules begin to be produced by ozone photolysis at the next vibrational level of $O_2(a^1\Delta_g, v)$ (Table 1).

The energy defect of reaction (6) is written as

$$\Delta E = E - E_{DO_3} - E_{1D} - E_{a0}, \quad (7)$$

where $E$ is the photon energy, $E_{DO_3}$ is the dissociation energy of the ozone molecule (1.05 eV), $E_{1D}$ is the energy of excitation of the $O(^1D)$ atom from the ground state of the oxygen atom (1.97 eV), and $E_{a0}$ is the energy of excitation of the level $O_2(a^1\Delta_g, v = 0)$ relative to the ground state of the oxygen molecule (0.977 eV).

The quantum yield of the $O_2(a^1\Delta_g, v)$ molecule is determined by the fraction of energy spent for exciting this level and is written as

$$\beta_{a, v}(x) = C_v x\left(1 - x - \frac{x^2}{2} - \frac{x^3}{2^2} - \frac{x^4}{2^3} - \ldots - \frac{x^v}{2^{v-1}}\right), \quad (8)$$

where the parameter

$$\bar{x} = \exp\left(-\frac{\Delta E}{E_{a0}}\right) \quad (9)$$

determines the fraction of $O_2(a^1\Delta_g, v)$ molecules having an energy above the excitation threshold of this level (here, $\Delta E$ is from (7)) and

$$C_v = \frac{1 - C_0 x_v - C_1 x_v(1 - x_v) - C_2 x_v\left(1 - x_v - \frac{x_v^2}{2}\right) - \ldots - C_{v-1} x_v\left(1 - x_v - \frac{x_v^2}{2} - \ldots - \frac{x_v^{v-1}}{2^{v-2}}\right)}{x_v\left(1 - x_v - \frac{x_v^2}{2} - \ldots - \frac{x_v^v}{2^{v-1}}\right)} \quad (10)$$

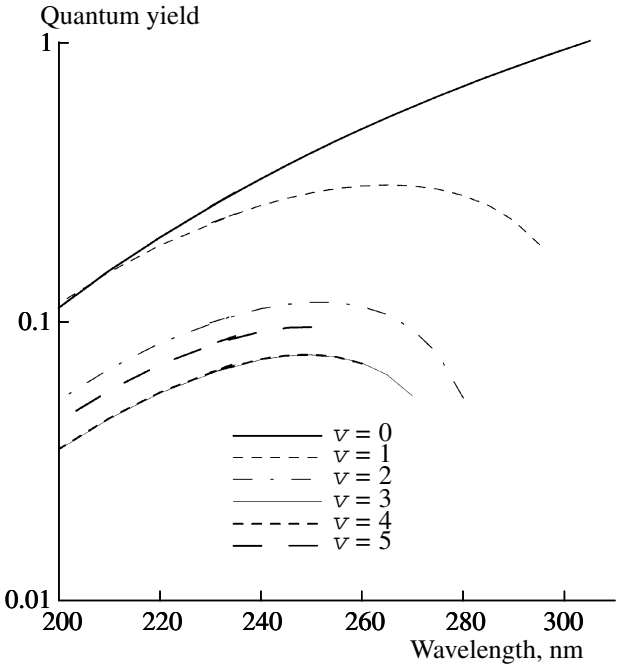


**Fig. 2.** Quantum yields of the production of electronically–vibrationally excited molecules of $O_2(a^1\Delta_g, v = 0–5)$ in the singlet channel of ozone photolysis in the Hartley band as a function of the wavelength.

is the normalization factor that is calculated such that the quantum yield of all electronically–vibrationally excited $O_2(a^1\Delta_g, v)$ molecules in a singlet channel (6) is unity,

$$\sum_{i=0}^{v} \beta_{a,v}(x_i) = 1. \quad (11)$$

Each normalization factor $C_v$ (for the $v$ level) was calculated for the threshold energy $x_v$ at which oxygen molecules begin to be formed by ozone photolysis at the next vibrational level (Table 1). The values of $x_v$ and normalization factors $C_v$ (from (10)) for the corresponding vibrational levels of $O_2(a^1\Delta_g, v)$ are listed in Table 1.

The approximation curves of quantum yields $\beta_{a,v}$ (8) generally agree well with the known experimental data for all $v = 0–5$. Typically, $v = 0$ for $\beta_{a,0}$ drops off monotonically with decreasing $\lambda$ and has a maximum for $v > 0$. Such a behavior also agrees with experimental data (Fig. 2). The proposed analytical formulas (8) fit the available experimental data fairly well for the higher values $v = 6$ and 7 [25], but, since there are only single measurements for these cases, they are not shown in Fig. 2.

## 3. USE OF THE YM-2003 MODEL

The YM-2003 model of the electronic–vibrational kinetics of $O_2$ and $O_3$ permits the following:

1. To solve a direct problem, i.e., to calculate the vertical profiles of concentrations of $O_2(b^1\Sigma_g^+, v \le 2)$, $O_2(a^1\Delta_g, v \le 5)$, and $O_2(X^3\Sigma_g^-, v \le 35)$ in the middle atmosphere. Emission intensities are calculated in the bands of oxygen molecules produced both by transitions from the vibrationally unexcited states $O_2(b^1\Sigma_g^+, v = 0)$ in the Atm (0–0) and $O_2(a^1\Delta_g, v = 0)$ in the IR Atm bands and by transitions from the electronically–vibrationally excited states $O_2(a^1\Delta_g, v = 1–5)$ and $O_2(b^1\Sigma_g^+, v = 1, 2)$, for example, $O_2(b^1\Sigma_g^+, v = 1) \longrightarrow O_2(X^3\Sigma_g^-, v = 0)$ (689 nm) and $O_2(b^1\Sigma_g^+, v = 2) \longrightarrow O_2(X^3\Sigma_g^-, v = 0)$ (629 nm).

2. To solve an inverse problem of the retrieval of the altitude profile of ozone concentration from measured emission intensities from both the vibrationally unexcited states ($v = 0$) and the states $O_2(b^1\Sigma_g^+, v > 0)$ and $O_2(a^1\Delta_g, v > 0)$, including the 689- and 629-nm emissions.

### *3.1. Mathematical Aspects of Solution of the Direct Problem*

The photodissociation of ozone and molecular oxygen produces excited oxygen atoms $O(^1D)$ and oxygen molecules in three electronically excited states $O_2(b^1\Sigma_g^+, v = 0–2)$, $O_2(a^1\Delta_g, v = 0–5)$, and $O_2(X^3\Sigma_g^-, v = 1–35)$. For all these 45 variables, which are the populations of the excited levels of atomic and molecular oxygen and are interrelated by photochemical reactions, a system of 45 first-order kinetic equations is solved for fixed altitudes in the range 65 to 125 km:

$$\frac{\partial n_i}{\partial t} = \sum_{k \ne i} (n_k p_{i,k}) - n_i q_i + P_i, \quad (12)$$

where $i$ is the level number ($i = 1–45$), $n_i$ is the population of the $i$th level, $p_{i,k}$ is the production rate of the $i$th component out of $k$ components ($k = 1–45$, $k \ne i$) in collisional processes of energy transfer, $q_i$ is the total quenching of the component $i$ in processes of collisional and radiative quenching, $P_i$ is the production rate for the $i$th component in the photolysis of $O_2$ and $O_3$ molecules (see (3)) and in chemical reactions (e.g., in collisional reactions of O with $O_3$).

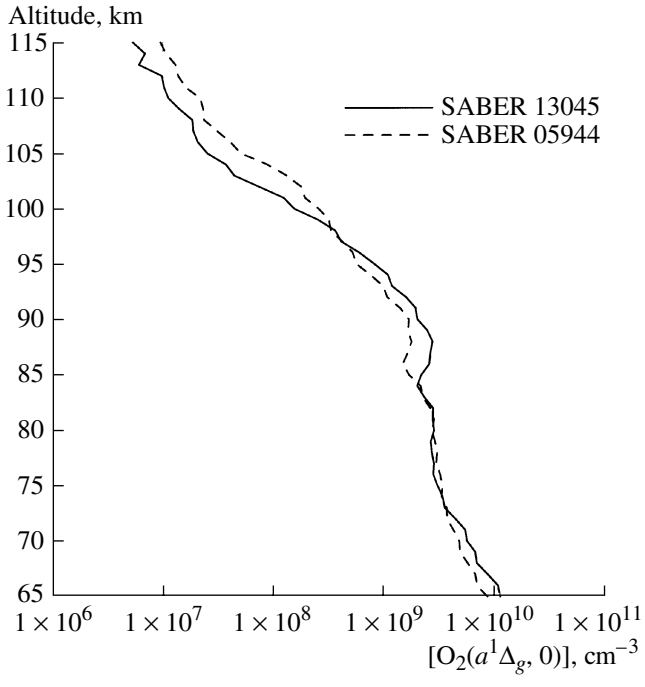


**Fig. 3.** Vertical profiles of $O_2(a^1\Delta_g, v = 0)$ retrieved from altitude profiles of emission intensities in the IR Atm $O_2$ band derived from measurements on slant paths in the SABER satellite experiment for episodes 13045 and 05944.

System of differential equations (12) can be written as a matrix equation for the vector of the level population $n$

$$\frac{\partial n}{\partial t} = \mathbf{A}n + P. \quad (13)$$

In a stationary case, system (13) can be written as a system of algebraic equations

$$n = -\mathbf{A}^{-1}P, \quad (14)$$

where **A** is a quasi-diagonal essentially sparse matrix. The method of solution of such systems of equations is described in [26].

The solution algorithm of (13) in a nonstationary case is under development.

Examples of calculation of the altitude profiles of the populations of electronically–vibrationally excited states of molecules $O_2(b^1\Sigma_g^+, v = 0–2)$, $O_2(a^1\Delta_g, v = 0–5)$, and $O_2(X^3\Sigma_g^-, v = 1)$ are given in [1, 2]. An additional result of the solution to the direct problem is presented in [27], namely, the calculation of the efficiency of thermalization of the excited products of molecular oxygen and ozone photolysis in the middle atmosphere with consideration for the energy transfer between the excited $O(^1D)$ atoms and electronically–vibrationally excited molecules of oxygen.

### *3.2. Solution of the Inverse Problem*

Taking into account the electronic–vibrational kinetics of the products of ozone and molecular oxygen photolysis becomes important for ozone-concentration retrieval from measured vertical profiles of Atm and IR Atm oxygen band emissions above 65 km. The use of the models of electronic–vibrational kinetics (YM-2003) and electronic kinetics (MSZ) leads to different altitude profiles of ozone concentration during the interpretation of measurements of the 762-nm and $O_2$ emissions.

We have used the models of electronic–vibrational and pure electronic kinetics for interpretation of the TIMED-SABER experimental data, which have become available for analysis since the summer of 2006. The satellite was launched in 2001, and measurements in ten broadband IR channels have been successfully continued. Channel 10 of the SABER instrument is centered at 1.27 μm; the transmission band of the filter includes the entire spectral interval of the IR Atm band [28]. We have used the data of measurements of the 1.27-μm emission of $O_2$ on slant paths in the TIMED-SABER satellite experiment for episodes 05944 and 13045, which are given at the official SABER Web site (version 1.06). The retrieved vertical profiles of the concentrations of $O_2(a^1\Delta_g, v = 0)$ are shown in Fig. 3. For the retrieval of the concentrations of $O_2(a^1\Delta_g, v = 0)$, we used the approximation of an optically thin atmosphere, which holds above 65 km according to our estimates.

The inverse problem of the retrieval of altitude profiles of ozone concentrations from altitude profiles of the volume emission rates in the 1.27-μm band was solved via our model of electronic–vibrational kinetics (YM-2003) and the electronic MSZ model, which remain to be used for processing TIMED-SABER data. The model of the atmosphere (including altitude profiles of molecular and atomic oxygen and of the gas temperature) was taken from the SABER atmospheric model.

We have processed a series of episodes for daytime and twilight conditions. The results of calculations for two typical episodes (05944 and 13045) are shown in Fig. 4 along with altitude ozone profiles retrieved by the MSZ model and with altitude ozone profiles retrieved from measured intensities of the $O_3$ 9.6-μm emission, available at the SABER website.

As can be seen in Fig. 4, the retrieved altitude profiles of the ozone concentration in the YM-2003 model of electronic–vibrational kinetics and in the MSZ model of pure electronic kinetics in the altitude range 70–85 km differ widely. The MSZ model gives an underestimated ozone abundance in comparison with YM-2003 throughout the entire altitude range, in agreement with results of the numerical experiment [2], the maximum difference between ozone concen-

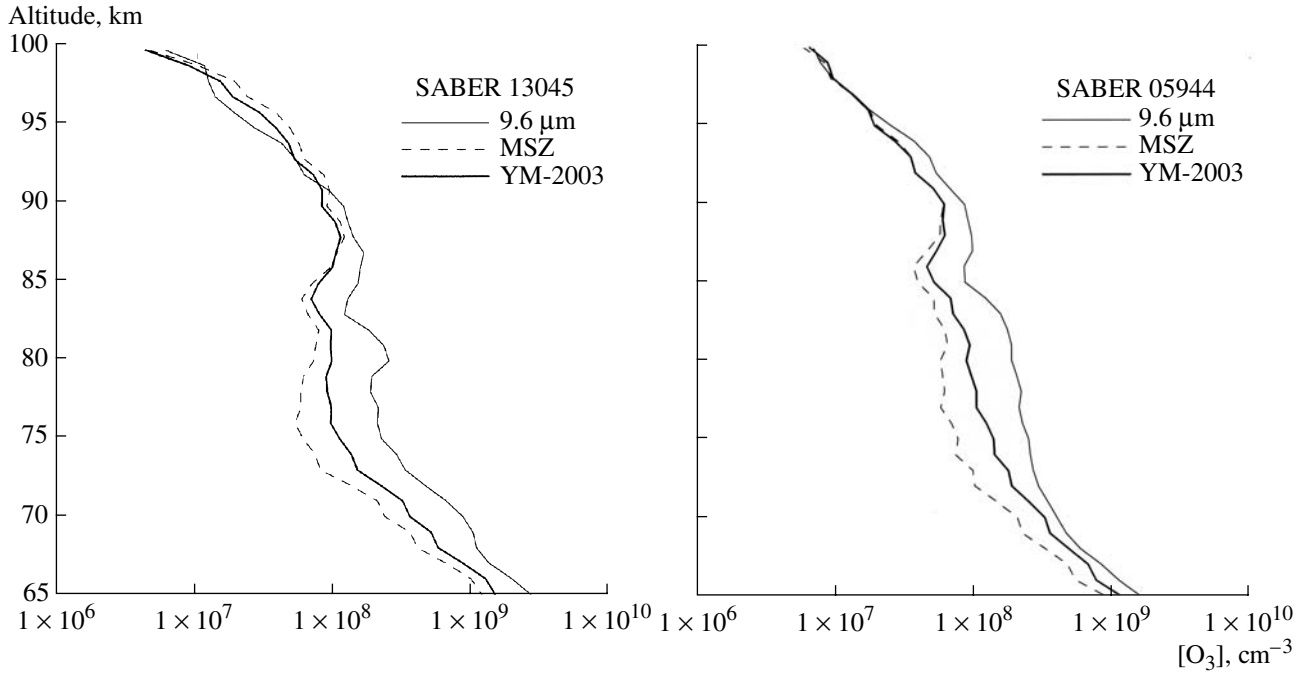


**Fig. 4.** Vertical ozone profiles retrieved from altitude profiles of the $O_2$ volume emission rates at 1.27 μm (Fig. 3) in MZS and YM-2003 and at 9.6 μm (SABER experiment).

trations being 46% per 75 km (episode 13045) and 47% per 74 km (episode 05944).

As evident from Fig. 4, the ozone concentrations in the interval 65–90 km that are retrieved from the SABER data in the channel of measurement of intensity in the 9.6-μm ozone band are much higher than those retrieved from the SABER data in the 1.27-2-μm channel. The maximum difference between the ozone concentrations retrieved from the IR Atm emission of the $O_2$ band (within the framework of the electronic–vibrational kinetics model YM-2003) and from the emission in the 9.6-μm band of $O_3$ is observed at 80 km, where the ozone concentrations differ by a factor of 2.2 (measurement 05944) and 2.6 (measurement 13045).

The causes of this discrepancy are difficult to explain unambiguously, because there are no publications on the interpretation of the SABER 9.6-μm channel and we do not know with certainty which model of the ozone vibrational kinetics was used for interpretation of measurements. Nonetheless, some suggestions can be made. As follows from the preliminary publication on this subject in 1998 [29], in the model of the vibrational kinetics of ozone molecules, 62 vibrational states of the $O_3$ molecule were taken into account and the assumption was made that the ozone molecule is excited to the levels with energies of about 5500 $cm^{-1}$. For the rate constants of collisional reactions between the vibrationally excited molecules of $O_3(v_1, v_2, v_3)$ and molecules of the atmospheric gases in accordance with the so-called "energy-gap" model, a unified formula was introduced. In this case, the rate constant of transition between vibrational states was taken to depend on the difference of energies between the initial and final states of the transition. The drawbacks of such models are their discrepancies with the actual kinetics of the lower vibrational states of the ozone molecule (up to energies of about 3000 $cm^{-1}$), the kinetics of which has been investigated sufficiently well in a series of experimental studies (e.g., [30, 31]), and of the upper vibrational states of the ozone molecule (up to the dissociation limit 8500 $cm^{-1}$), which belong to the region of vibrational quasi-continuum [32]. Therefore, the model of vibrational kinetics proposed in [29] has become obsolete, and López-Puertas and Taylor's model was most likely used for interpretation of the experiment [33] (see below).

In the experiment of [32], it has been found that the recombination reaction produces highly excited ozone molecules in vibrational states that are close in energy to the dissociation energy of the molecule (about 8500 $cm^{-1}$) and that vibrational states with energies greater than the energy of the level tetrad (003, 102, 201, 300) lie in the vibrational quasi-continuum. The physics of the vibrational quasi-continuum is very complicated, and the theory of such a set of states that are closely spaced by energy is a matter of the future; however, it is clear that transitions between the states in this region cannot be described by the rate constants of reactions. That is the reason the model of the ozone

vibrational kinetics introduced by Manuilova and Shved in 1992 [34] included 20 vibrational states of the ozone molecule up to the tetrad levels (003, 102, 201, 300) and the recombination reaction was assumed to produce vibrationally excited ozone in one of the states of the given tetrad. The rate constants of collisional transitions between vibrational states were obtained from experimental data, mainly from the results of [30, 31]. In 1998 [35], we have supplemented the model by another three vibrational states 040, 031, and 130 and updated the database of the rate constants of collisional reactions, with inclusion of spectroscopic information according to recent experimental data. Our model was used by Kaufmann et al. in 2002 for the interpretation of 9.6-μm measurements in the CRISTA experiment [36].

The model of ozone vibrational kinetics, a hybrid from our model of the lower vibrational states and the model where the upper states of the vibrational quasi-continuum are taken into account with the use of a unified formula for the rate constants of collisional reactions, has been described in monograph [33]. A similar model was used for the interpretation of measurements with a high-resolution (0.035 $cm^{-1}$) MIPAS instrument during an experiment onboard the ENVISAT satellite in narrow spectral regions (microwindows) in the 9.6- and 4.8-μm ozone bands [37, 38]. In [37], ozone was assumed to be formed at levels with energies close to the dissociation limit of 8500 $cm^{-1}$ and 250 vibrational states were considered. The altitude profiles of ozone were determined from measurements in microwindows of the spectral region of the "first-level vibrational excitation" transitions 010–000, 100–000, and 001–000, where the hot bands make the least contribution. Therefore, the altitude ozone profile up to 70–75 km was determined to within about 10% [37]. These altitude profiles were used for interpretation of measurements in microwindows lying in the 4.8-μm ozone band [38]. However, an attempt to use the vibrational kinetics model to interpret measurements in this ozone band, which is formed mainly by transitions from the "second-level vibrational excitation" triad states (200, 101, 002) to the ground vibrational level, has failed. The result of using this model was that the 4.8-μm emission intensity calculated for a given altitude profile of ozone concentration turned out to be two to three times lower than that measured in the altitude interval of 50 to 75 km. This fact is explained by an underestimation of the populations of states (200, 101, and 002). This result establishes that, under non-LTE conditions, the given model produces underestimated populations of both the upper and the lower vibrational states [34, 35], including states 010, 100, and 001, and, consequently, the ozone 4.8- and 9.6-μm emissions will likewise be strongly underestimated. Hence, the ozone concentration retrieved from measurements in the 9.6-μm band in this model will be substantially overestimated. For an adequate interpretation of the experiment in the 4.8-μm band, the authors of [38] have had to assume that either ozone is formed in one of the states of a tetrad (003, 102, 201, 300) in the region of energy 3000 $cm^{-1}$ or that the rate constant of the collisional transitions of energy exchange between the bending and stretching modes is three to four times lower than its well-known value determined from experiments. Since the latter assumption is unlikely, the former has to be used. Thus, an attempt to take into account the quasi-continuum of ozone simply with no relation to the complex physics of this phenomenon has failed, and, for an adequate interpretation of MIPAS measurements in the 4.8-μm ozone band, the model of ozone vibrational kinetics developed in 1992–1998 has to be used [34, 35].

As can be seen from the large difference between ozone concentrations retrieved from the interpretation of measurements at 1.27 μm and 9.6 μm, SABER measurements in the ozone 9.6-μm band have been interpreted via a model of the ozone vibrational kinetics that is similar to that described in [33]. In this model, ozone is assumed to be vibrationally excited to the levels with an energy close to the dissociation limit and, consequently, the contribution of hot-band transitions to the total 9.6 μm band intensity is assumed to be significant. Note that microwindows for the high-resolution MIPAS were chosen with a frequency interval such that the contribution of hot-band transitions from the upper excited vibrational states was as small as possible up to altitudes of 70 to 75 km. However, in addition to the main 001–000 and 100–000 transitions, a contribution to the emission measured in the SABER 9.6-μm channel with a spectral interval of 1010–1140 $cm^{-1}$ [28] comes from at least 17 hot-band transitions [29]. As was noted above, López-Puertas and Taylor's model should produce underestimated populations of all vibrational excited states and, consequently, strongly oversized ozone concentrations in the region of the maximum deviation from LTE in vibrational states. Therefore, the large difference between altitude profiles of ozone in Fig. 4 in the altitude range 70–90 km is quite explicable.

## 4. ANALYSIS OF THE SENSITIVITY OF THE YM-2003 MODEL

### *4.1. Problem Formulation and Main Results*

In a general case, concentrations of excited components calculated with a model of ozone and molecular oxygen photodissociation depend on all of the parameters involved in this model: concentrations of atmospheric components, photodissociation rates, rate constants of reactions, and quantum yields of the products in these reactions. Denote these input parameters by $x_i$ and the required function by $f$. Then, the variation of

**Table 2.** Rate constants of the most important reactions for the YM-2003 model

| Reaction | Rate constant, $K$ ($cm^3\ s^{-1}$) | Reference |
|---|---|---|
| $O(^1D) + O_2 \longrightarrow$ products | $k_I = (3.12 \pm 0.25) \times 10^{-11} e^{(70 \pm 10)/T}$ | [40] |
| $O(^1D) + N_2 \longrightarrow$ products | $k_{II} = (2.1 \pm 0.2) \times 10^{-11}\ e^{(115 \pm 10)/T}$ | [40] |
| $O_2(b, 1) + O_2 \longrightarrow O_2(X, 1) + O_2(b, 0)$ | $k_{III} = (2.2 \pm 0.8) \times 10^{-11} (T/292)^{1.0 \pm 0.3} e^{-(115 \pm 105)/T}$ | [7] |
| $O_2(b, 0) + N_2 \longrightarrow$ products | $k_{IV} = (2.03 \pm 0.30) \times 10^{-15} e^{-(37 \pm 40)/T}$ | [9, 41] |
| $O_2(b, 0) + CO_2 \longrightarrow O_2(a, 0) + CO_2$ | $k_V = (3.39 \pm 0.36) \times 10^{-13}$ | [9] |

Note: $O_2(b^1\Sigma_g^+, v)$, is denoted as $O_2(b, v)$, $O_2(a^1\Delta_g, v)$, is denoted as $O_2(a, v)$, and $O_2(X^3\Sigma_g^-, v)$, is denoted as $O_2(X, v)$.

the required function $f$ during small changes in the input parameters can be written as

$$df = \sum_i \frac{\partial f}{\partial x_i} dx_i, \tag{15}$$

where summation is made over all input parameters.

From (15), we obtain the relative error of $f$ as a function of the relative errors of the input parameters $x_i$:

$$\frac{df}{f} = \sum_i \frac{\partial f}{\partial x_i} \frac{dx_i}{f} = \sum_i \frac{\partial \ln f}{\partial \ln x_i} \frac{dx_i}{x_i}, \tag{16}$$

where $\frac{\partial \ln f}{\partial \ln x_i}$ is the sensitivity coefficient $S_i$ of the required function $f$ versus the variation of the input parameter $x_i$ provided all other parameters $x_j$ for $j \neq i$ are kept constant, and $\frac{dx_i}{x_i}$ is the relative error $\delta_i$ in prescribing the input parameter $x_i$.

Thus, for small variations in the input parameters under consideration, formula (16) has a simple physical interpretation. The relative error of the output parameter $f$ is related to the relative errors of the input parameters $x_i$ and to the sensitivity coefficients $S_i$, which describe the properties of the photodissociation model of ozone and molecular oxygen:

$$\frac{\Delta f}{f} = \sum_i S_i \delta_i. \tag{17}$$

The sensitivity coefficient $S_i$ is a dimensionless number that shows how strongly the required parameter $f$ depends on the variation in the input parameter $x_i$, it is assumed that $|S| > 1.0$ means strong sensitivity, $0.1 < |S| < 1.0$ is normal sensitivity, and $|S| < 0.1$ is weak sensitivity.

It should be noted that, if the sensitivity $S_i$ to variations in any of the input parameters (chemical-reaction rate constant $k_i$; atmospheric constituents $[O_2]$, $[N_2]$, $[O(^3P)]$, $[O_3]$, and $[CO_2]$; or gas temperature $T_g$) is low, it does not mean that the given parameter is unimportant and can be eliminated from the total list of the reactions included in the model, because this parameter may have a large relative error $\delta_i$. There are processes whose dimensionless sensitivity is weak in a direct problem (calculation of the profiles of $O_2(b^1\Sigma_g^+, v)$, $O_2(a^1\Delta_g, v)$), but they cannot be disregarded in an inverse problem ($O_3$ retrieval).

Within the framework of the YM-2003 model, the sensitivity of the model was tested in the direct problem of

(a) calculation of the concentration of $O_2(b^1\Sigma_g^+, v)$ and

(b) calculation of the concentration of $O_2(a^1\Delta_g, v)$;

and in the inverse problem of

(c) retrieval of the vertical profile of $O_3$ from the Atm (0–0) emission of the $O_2$ band and

(d) retrieval of the vertical profile of $O_3$ from the Atm (0-0) emission of the $O_2$ band for variations in the concentrations of the atmospheric constituents $[O_2]$, $[N_2]$, $[O(^3P)]$, $[O_3]$, and $[CO_2]$; gas temperature $T_g$; and rate constants of reactions.

As a result of YM-2003 sensitivity analysis, the atmospheric constituents and reactions that have influence on calculations in the direct and inverse problems have been determined. The rate constants of the most important reactions are given in Table 2. A more detailed model-sensitivity analysis can be found in [39].

The constant rates except for $k_{III}$ were measured with a sufficiently high accuracy. The rate constants $k_I$, $k_{II}$, $k_{IV}$, and $k_V$ were measured with an error within 20%, and only the rate constant $k_{III}$ had an error $\delta$ of 37%. However, the contribution of the reaction $O_2(b^1\Sigma_g^+, v = 1) + O_2 \longrightarrow O_2(X^3\Sigma_g^-, v = 1) + O_2(b^1\Sigma_g^+, v = 0)$ in the direct problem is significant (e.g., the sensitivity coefficient lies within $0.62 < |S_{III}| < 0.87$ in the altitude interval from 60 to 100 km and $S_{III}\delta_{III} = 0.30$ at the mesopause).

The reaction $O(^1D) + O_2$ is the main source of $O_2(b^1\Sigma_g^+, v = 0)$ and, consequently, of the daytime mesospheric and lower-thermosphere 762-μm emission airglow in the transition $O_2(b^1\Sigma_g^+, v = 0) \longrightarrow O_2(X^3\Sigma_g^-, v = 0)$. Its rate constant $k_I$ is now well known (the error does not exceed 8%), and the sensitivity coefficient in the altitude range 60–100 km lies within $0.22 < |S_I| < 0.68$.

At altitudes between 60 and 100 km, the sensitivity of the model to variations in the rate constant of the reaction $O(^1D) + N_2 \longrightarrow$ is within $0.72 < |S_{II}| < 1.51$, and this reaction might have had a significant influence on daytime mesospheric and lower-thermosphere ozone retrieval from the 762-nm emission in the daytime mesosphere and lower thermosphere. However, the error of the rate constant of this reaction does not exceed 9% (Table 2); therefore, the error of ozone retrieval in the middle atmosphere due to variations in the rate constant of this reaction is $S_{II}\delta_{II} = 0.06–0.14$.

The quenching of $O_2(b^1\Sigma_g^+, v = 0)$ by molecular nitrogen $N_2$ is a key reaction in the retrieval of ozone from the emission intensity at 1.27 μm because the rate constant of this reaction is almost 100 times higher than the rate constant of the deactivation of $O_2(b^1\Sigma_g^+, v = 0)$ by $O_2$. Typical values of the sensitivity coefficient at 60–100 km lie in the range $0.1 < |S_{IV}| < 0.9$. The error of mesospheric ozone retrieval caused by variations in the rate constant of this reaction is $S_{IV}\delta_{IV} = 0.13–0.48$. The results of the inverse problem are significantly affected not only by the rate constant of reaction but also by the quantum yield of the products in this reaction (see Section 4.2).

Although $CO_2$ is a minor constituent of the atmosphere, variations in the rate constant of the reaction $O_2(b^1\Sigma_g^+, v = 0) + CO_2 \longrightarrow O_2(a^1\Delta_g, v = 0) + CO_2$ affect the retrieval of the vertical profile of $O_3$ because the rate constant of this reaction is two orders of magnitude higher than the rate constant of $O_2(b^1\Sigma_g^+, v = 0) + N_2$. Typical values of the sensitivity coefficient at 60–100 km are within $0.02 < |S_V| < 0.28$.

### *4.2. Dependence of Vertical Ozone Profile Retrieval on Quantum Yields of the Products of the Quenching of $O_2(b^1\Sigma_g^+, v = 0)$ by Molecular Nitrogen*

For the quenching of $O_2(b^1\Sigma_g^+, v = 0)$ by molecular nitrogen $N_2$, there is a problem of calculating the quantum yields of products. In the MSZ model, it is assumed that the quantum yield of $O_2(a^1\Delta_g, v = 0)$ in the reaction

$$O_2(b^1\Sigma_g^+, v = 0) + N_2 \longrightarrow O_2(a^1\Delta_g, v = 0) + N_2(X, v = 2) + 607.1\ \text{cm}^{-1} \quad (18)$$

is unity [11]. Within the framework of the YM-2003 model of the $O_2$ and $O_3$ electronic–vibrational kinetics, different possible pathways of the quenching of $O_2(b^1\Sigma_g^+, v = 0)$ by $N_2$ molecules were considered. Because of a relatively large value of the constant rate of this reaction, it was assumed in [41] that the process follows the pattern of a quasi-resonance process:

$$O_2(b^1\Sigma_g^+, v = 0) + N_2 \longrightarrow O_2(a^1\Delta_g, v = 2) + N_2(X, v = 1) - 31.9\ \text{cm}^{-1}. \quad (19)$$

One more quasi-resonance process is possible, namely,

$$O_2(b^1\Sigma_g^+, v = 0) + N_2 \longrightarrow O_2(X^3\Sigma_g^-, v = 9) + N_2(X, v = 0) - 52.8\ \text{cm}^{-1}. \quad (20)$$

At present, there is no information on possible quantum yields of the products of this reaction in channels (19) and (20). We assumed that these channels have equal values of quantum yields [2]. In the given paper (Fig. 5), we performed calculations of vertical ozone profiles for three values of the quantum yield of reaction (19) for conditions of the experiment (SABER, measurement 13045). At 75 km, the value of quantum yield has the largest effect on ozone: the ozone concentration differs from the standard variant (quantum yield $\beta_{19} = 0.5$) by about ±19% when $\beta_{19}$ is varied by ±40%

## 5. CONCLUSIONS

1. The model of $O_2$ and $O_3$ electronic–vibrational kinetics computes emission intensities in the oxygen bands produced both by transitions from the states unexcited in vibrational degrees of freedom $O_2(a^1\Delta_g, v = 0)$ (1.27 μm) and $O_2(b^1\Sigma_g^+, v = 0)$ (762 nm) and by transitions from the electronic–vibrational states $O_2(a^1\Delta_g, v = 1–5)$ and $O_2(b^1\Sigma_g^+, v = 1, 2)$ ($O_2(b^1\Sigma_g^+, v = 1) \longrightarrow O_2(X^3\Sigma_g^-, v = 0)$ (689 nm), $O_2(b^1\Sigma_g^+, v = 2) \longrightarrow O_2(X^3\Sigma_g^-, v = 0)$ (629 nm). This provides the possibility for retrieval of vertical ozone profiles from the last two emissions.

2. Ozone retrieval from the TIMED-SABER measurements of emission intensities at 1.27 μm in the model of electronic–vibrational kinetics and in the model of electronic kinetics of ozone and molecular

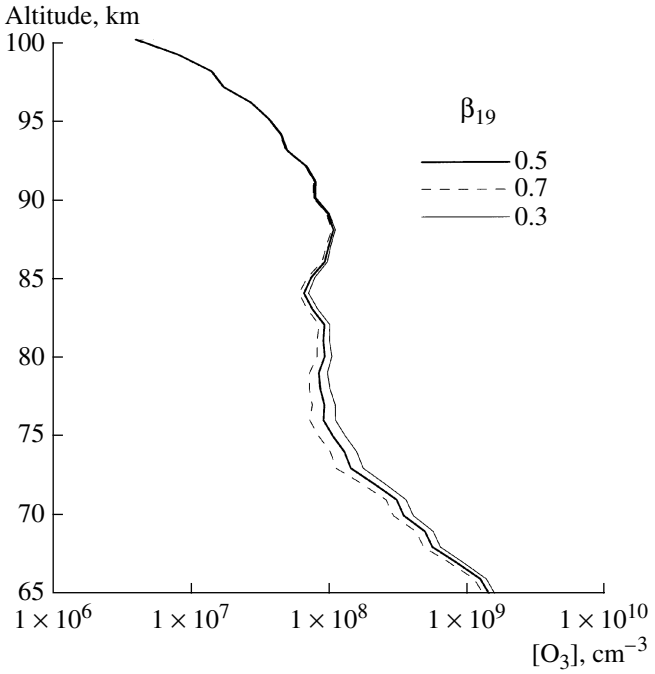


**Fig. 5.** Vertical ozone profiles retrieved from altitude profiles of the $O_2$ volume emission rates at 1.27 μm (Fig. 3) in the YM-2003 model for three values of the quantum yield of $O_2(a^1\Delta_g, v = 2)$ molecules in the reaction $O_2(b^1\Sigma_g^+, v = 0) + N_2 \longrightarrow$ for the experiment (SABER 13045).

oxygen photolysis gives different results. Ozone concentrations retrieved in the model of electronic kinetics (MSZ) are lower than those derived from the YM-2003 model. The difference reaches 47% at about 75 km.

## ACKNOWLEDGMENTS

We thank I.V. Olemskoi for help with development of calculation algorithms.

The study was supported in part by the Russian Foundation for Basic Research, project no. 05-05-65318.

## REFERENCES

1. V. A. Yankovsky and R. O. Manuilova, "New Self-Consistent Model of the Diurnal Emissions $O_2(a^1\Delta_g, v)$ and $O_2(b^1\Sigma_g^+, v)$ in the Middle Atmosphere: Retrieval of the Vertical Profile of Ozone from the Measured Profiles of the Intensity of These Emissions," Opt. Atmos. Okeana **16**, 582–586 (2003).
2. V. A. Yankovsky and R. O. Manuilova, "Model of Daytime Emissions of Electronically–Vibrationally Excited Products of $O_3$ and $O_2$ Photolysis: Application to Ozone Retrieval," Ann. Geophys. **24**, 2823–2839 (2006).
3. L. E. Khvorostovskaya and V. A. Yankovsky, "On a Mechanism of Ozone Formation in Molecular-Oxygen Glow Discharge," Opt. Spektrosk. **37** (1), 26–30 (1974).
4. L. E. Khvorostovskaya and V. A. Yankovsky, "Experimental Study of Processes with Participation of Metastable Atoms and Molecules in Oxygen Glow Discharge," Khim. Fiz. **3**, 1561–1572 (1984).
5. L. E. Khvorostovskaya and V. A. Yankovsky, "Negative Ions, Ozone and Metastable Components in DC Oxygen Glow Discharge," Contr. Plasm. Phys. **31**, 71–88 (1991).
6. V. A. Yankovsky, "Electronic–Vibrational Relaxation of $O_2(b^1\Sigma_g^+, v = 1, 2)$ Molecules in Collisions with Ozone and with Oxygen Molecules and Atoms," Khim. Fiz. **10**, 291–306 (1991).
7. T. G. Slanger and R. A. Copeland, "Energetic Oxygen in the Upper Atmosphere and the Laboratory," Chem. Rev. **103**, 4731–4765 (2003).
8. D. A. Pejakovic, E. R. Wouters, K. E. Phillips, et al., "Collisional Removal of by $O_2$ at Thermospheric Temperatures," J. Geophys. Res. A **110**, 03308, doi: 10.1029/2004JA010860 (2005).
9. W. B. DeMore, D. M. Golden, R. F. Hampson, et al., "Chemical Kinetics and Photochemical Data for Use in Stratospheric Modeling," JPL Publ. **97-4**, 1–128 (1997).
10. M. G. Mlynczak, F. Morgan, and J.-H. Yee, "Simultaneous Measurements of the $O_2(a^1\Delta_g)$ and $O_2(b^1\Sigma_g^+)$ Airglows and Ozone in the Daytime Mesosphere," Geophys. Rev. Lett. **28**, 999–1002 (2001).
11. M. G. Mlynczak, S. C. Solomon, and D. S. Zaras, "An Updated Model for $O_2(a^1\Delta_g)$ Concentrations in the Mesosphere and Lower Mesosphere and Implications for Remote Sensing of Ozone at 1.27 μm," J. Geophys. Res. D **98**, 18 639–18 648 (1993).
12. R. Atkinson, D. L. Baulch, R. A. Cox, et al., "Evaluated Kinetic and Photochemical Data for Atmospheric Chemistry Supplement VI. IUPAC Subcommittee on Gas Kinetic Data Evaluation for Atmospheric Chemistry," J. Phys. Chem. Ref. Data **26**, 1329–1497 (1997).
13. W. K. Tobiska, T. Woods, F. Eparvier, et al., "The SOLAR2000 Empirical Solar Irradiance Model and Forecast Tool," J. Atmos. Solar Terr. Phys **62**, 1233–1250 (2000).
14. W. K. Tobiska and S. D. Bouwer, "New Developments in SOLAR2000 for Space Research and Operations," Adv. Space Res. **37**, 347–358 (2006).
15. K. Yoshino, W. H. Parkinson, K. Itob, et al., "Absolute Absorption Cross Section Measurements of Schumann–Runge Continuum of $O_2$ at 90 and 295 K," J. Mol. Spectrosc. **229**, 238–243, doi: 10.1016/j.jms.2004.08.020 (2004).
16. S. P. Sander, R. R. Friedl, A. R. Ravishankara, et al., "Chemical Kinetics and Photochemical Data for Use in Atmospheric Studies," JPL Publ. **02-25**, Evaluation Number 14 (2003).
17. G. Kockarts, "Penetration of Solar Radiation in the Schumann–Runge Bands of Molecular Oxygen: A Robust Approximation," Ann. Geophys. **12**, 1207–1217 (1994).

18. T. Reddmann and R. Uhl, "The H Lyman-α Actinic Flux in the Middle Atmosphere," Atmos. Chem. Phys. **3**, 225–231 (2003).
19. *Atmospheric Ozone 1985—Assessment of Our Understanding of the Processes Controlling Its Present Distribution and Change*, WMO Global Ozone Research Monitoring Project Report No. 16 (WMO, Geneva, 1986).
20. E. J. Llewellyn and I. C. McDade, "A Reference Model for Atomic Oxygen in the Terrestrial Atmosphere," Adv. Space Res. **18** (9/10), 209–226 (1996).
21. R. Rodrigo, J. J. López-Moreno, M. López-Puertas, et al., Neutral Atmospheric Composition between 60 and 220 km: A Theoretical Model for Mid-Latitudes," Planet. Space Sci. **34**, 723–743 (1986).
22. G. M. Keating and C. Chen, "Extensions to the CIRA Reference Models for Middle Atmosphere Ozone," Adv. Spane Res. **13**, 45–54 (1993).
23. A. E. Hedin, "Extension of the MSIS Thermosphere Model into the Middle and Lower Atmosphere," J. Geophys. Res. A **96**, 1159–1172 (1991).
24. V. A. Yankovsky and V. A. Kuleshova, "Photodissociation of Ozone in the Hartley Band: Analytic Description of $O_2(a^1\Delta_g, v = 0–3)$ Quantum Yields Depending on the Wavelength," Opt. Atmos. Okeana **19**, 576–580 (2006).
25. S. M. Dylewski, J. D. Geiser, and P. L. Houston, "The Energy Distribution, Angular Distribution, and Alignment of the$O(^1D_2)$ Fragment from the Photodissociation of Ozone between 235 and 305 nm," J. Chem. Phys. **115**, 7460–7473 (2001).
26. I. V. Olemskoi, "Modification of an Algorithm of Extracting Structural Features," Vestn. SPbGU, ser. 10, issue 2, 46–55 (2006).
27. V. A. Yankovsky, R. O. Manuilova, and V. A. Kuleshova, "Heating of the Middle Atmosphere As a Result of Quenching of the Products of$O_2$ and $O_3$ Photodissociation," Proc. SPIE—Int. Soc. Opt. Eng. **5743**, 34–40 (2004).
28. J. J. Tansock, S. Hansen, and K. Paskett, "SABER Ground Calibration," J. Remote Sensing **24**, 403–420 (2003).
29. M. G. Mlynczak and D. K. Zhou, "Kinetic and Spectroscopic Requirements for the Measurement of Mesospheric Ozone at 9.6 μm under Non-LTE Conditions," Geophys. Rev. Lett. **25**, 639–642 (1998).
30. F. Menard-Bourcin, L. Doyennete, and J. Menard, "Vibrational Energy Transfers in Ozone from Infrared Double-Resonance Measurements," J. Chem. Phys. **92**, 4212–4221 (1990).
31. F. Menard-Bourcin, L. Doyennete, and J. Menard, "Vibrational Energy Transfers in Ozone Excited Into the (101) State from Double-Resonance Measurements," J. Chem. Phys. **101**, 8636–8645 (1994).
32. J. A. Joens, J. B. Burkholder, and E. J. Bair, "Vibrational Relaxation in Ozone Recombination," J. Chem. Phys. **76**, 5902–5916 (1982).
33. M. López-Puertas and F. W. Taylor, *Non-LTE Radiative Transfer in the Atmosphere* (World Science Publ., Singapore, 2001).
34. R. O. Manuilova and G. M. Shved, "The 4.8 and 9.6 μm Ozone Band Emissions in the Middle Atmosphere," J. Atmos. Terr. Phys. **54**, 1149–1168 (1992).
35. R. O. Manuilova, O. A. Gusev, A. A. Kutepov, et al., "Modelling of Non-LTE Limb Spectra of IR Ozone Bands for the MIPAS Space Experiment," J. Quant. Spectrosc. Radiat. Transfer **59**, 405–422 (1998).
36. M. Kaufmann, O. A. Gusev, and K. U. Grossmann, "Satellite Observations of Day- and Nighttime Ozone in the Mesosphere and Lower Thermosphere," J. Geophys. Res. D **108**, 4272–4286 (2002).
37. S. Gil-López, M. López-Puertas, M. Kaufmann, et al., "Retrieval of Stratospheric and Mesospheric $O_3$ from High Resolution MIPAS Spectra at 15 and 10 μm," Advances Space Res. **36**, 943–951 (2005).
38. M. Kaufmann, S. Gil-López, M. López-Puertas, et al., "Vibrationally Excited Ozone in the Middle Atmosphere," J. Atmos. Solar–Terr. Phys. **68**, 202–212 (2006).
39. V. A. Kuleshova and V. A. Yankovsky, "Model of Electronic–Vibrational Kinetics of $O_2$ and $O_3$ Photolysis in the Earth's Middle Atmosphere: Analysis of Sensitivity," Opt. Atmos. Okeana **20** (in press).
40. G. E. Streit, C. J. Howard, A. L. Schmeltekopf, et al., "Temperature Dependence of $O(^1D)$ Rate Constants for Reactions with $O_2$, $N_2$, $CO_2$, $O_3$, $H_2O$," J. Chem. Phys. **65**, 4761–4764 (1976).
41. M. Braithwaite, J. A. Davidson, and E. A. Ogryzlo, "$O_2(b^1\Sigma_g^+)$ Relaxation in Collisions. I. The Influence of Long Range Forces in the Quenching by Diatomic Molecules," J. Chem. Phys. **65**, 771–778 (1976).